

Transient Capability of 3D MOC Code STREAM

Anisur Rahman, and Deokjung Lee

Department of Nuclear Engineering, Ulsan National Institute of Science and Technology
50 UNIST-gil, Ulsan, 44919, Republic of Korea

*Corresponding author: anisur@unist.ac.kr, deokjung@unist.ac.kr

1. Introduction

STREAM [1,2], A three-dimensional (3-D) method of characteristics (MOC) neutron transport code is used for light water nuclear reactor core analysis. The 3-D neutron transport model become popular for nuclear reactor analysis because of without approximation, availability of computer capability and more accurate results. General task of transport model is to solve time, energy and space dependent the Boltzmann neutron transport equation. In STREAM [2], 3-D Method of Characteristics/Diamond-difference (MOC/DD) method has been implemented to solve neutron transport equation in 2-D plane wise without any axial solver. STREAM library uses 72-groups in MOC while 8-groups for CMFD. It has pin-wise as well as assembly-wise CMFD solver. In CMFD solver, assembly-wise solver is used to accelerate pin-wise CMFD.

The time-dependent neutron flux is the product of two functions called ‘amplitude’ and ‘shape’. This report describes the MOC theory of transient to calculate the power shape function. In amplitude function STREAM used exact point-kinetic equation in amplitude function.

2. Method of Characteristics

2.1 MOC transient equation

The time dependent neutron transport equation along a characteristic line is

$$\frac{1}{\vartheta(E)} \frac{\partial \psi_{i,j,k}^g(s,z,t)}{\partial t} = -\cos \bar{\theta}_j \frac{\partial \psi_{i,j,k}^g(s,z,t)}{\partial s} - \sin \bar{\theta}_j \frac{\partial \psi_{i,j,k}^g(s,z,t)}{\partial z} - \Sigma_{tr,m}^g \psi_{i,j,k}^g(s,z,t) + \bar{Q}_{ij}^g(s,z,t) \quad (1)$$

where the isotropic neutron source is given as:

$$\bar{Q}_{ij}^g(s,z,t) = \frac{1}{4\pi} [\chi_{p,m}^g (1 - \beta) S_{F,m}(t) + \sum_{g'} \Sigma_{s,m}^{g' \rightarrow g} \phi_m^{g'}(t) + \chi_{d,m}^g S_{d,m}(t)] \quad (2)$$

where,

$\chi_{d,m}^g$ is the delayed neutron spectrum,

$$S_{F,m}(t) = \frac{1}{k_{eff}} \sum_{g'} v \Sigma_{f,m}^{g'} \phi_m^{g'}(t)$$

β is the total delayed neutron fraction,

$\vartheta(E)$ is the neutron velocity.

Typically, in nuclear reactor transient analysis, the number of delayed neutron precursor is six, and the delayed neutron precursors density for group k, $C_k(s,z,t)$, can be described by Eq. (16);

$$\frac{dC_k(s,z,t)}{dt} = \beta_k(s,z,t) S_F(s,z,t) - \lambda_k(s,z,t) C_k(s,z,t) \quad (3)$$

where,

λ_k is the delay constant for delayed neutron precursor group k,

C_k is the delayed neutron precursor concentration of group k,

β_k is the group k delayed neutron precursor yield and be assumed to be independent of time.

Rewrite Eq. (1), moving time dependent parameter to the right side

$$\cos \bar{\theta}_j \frac{\partial \psi_{i,j,k}^g(s,z,t)}{\partial s} + \sin \bar{\theta}_j \frac{\partial \psi_{i,j,k}^g(s,z,t)}{\partial z} + \Sigma_{tr,m}^g \psi_{i,j,k}^g(s,z,t) = \bar{Q}_{ij}^g(s,z,t) \quad (4)$$

$$\text{where, } \bar{Q}_{ij}^g(s,z,t) = \bar{Q}_{ij}^g(s,z,t) - \frac{1}{\vartheta(E)} \frac{\partial \psi_{i,j,k}^g(s,z,t)}{\partial t}$$

s is the radial coordinate in the x-y plane, z is the coordinate in the axial direct, i is the index of azimuthal angle, j is the index of polar angle, k is the index for ray segment, g is the index of energy group, m is the index for source region, $\Sigma_{tr,m}^g$ is the transport cross section at flat source region m.

Consider, 3-D flux and source are approximately combination of 2-D radial component and 1-D axial component.

$$\begin{aligned} \phi^g &\approx \bar{\phi}_m^g b(z) \\ \psi_{i,j,k}^g(s,z) &\approx \psi_{i,j,k}^g(s,z) b(z) \\ Q_{i,j}^g(s,z) &\approx Q_{i,j}^g(s,z) b(z) \end{aligned}$$

The axial-averaged flux and source are defined

$$\begin{cases} \psi_{i,j,k}^{g,0}(s) = \frac{1}{2} (\psi_{i,j,k}^{g,+}(s) + \psi_{i,j,k}^{g,-}(s)) \\ \bar{\phi}_m^{g,0} = \frac{1}{2} (\bar{\phi}_m^{g,+} + \bar{\phi}_m^{g,-}) \\ \bar{Q}_{i,j,m}^{g,0} = \frac{1}{2} (\bar{Q}_{i,j,m}^{g,+} + \bar{Q}_{i,j,m}^{g,-}) \end{cases}$$

where, z+ and z- are the upper and lower positions of the axial domain

Rewrite equation (4) and integrating over the axial domain:

$$\begin{aligned} \cos \bar{\theta}_j \frac{\partial \psi_{i,j,k}^{g,0}(s,t)}{\partial s} + \frac{\sin \bar{\theta}_j}{\Delta z} (\psi_{i,j,k}^{g,+}(s,t) - \psi_{i,j,k}^{g,-}(s,t)) + \Sigma_{tr,m}^g \psi_{i,j,k}^{g,0}(s,t) &= \bar{Q}_{ij}^{g,0}(s,t) \\ \cos \bar{\theta}_j \frac{\partial \psi_{i,j,k}^{g,0}(s,t)}{\partial s} + \frac{2 \sin \bar{\theta}_j}{\Delta z} \psi_{i,j,k}^{g,0}(s,t) + \Sigma_{tr,m}^g \psi_{i,j,k}^{g,0}(s,t) &= \bar{Q}_{i,j,m}^{g,0} + \frac{2 \sin \bar{\theta}_j}{\Delta z} \psi_{i,j,k}^{g,-}(s,t) \end{aligned} \quad (5)$$

For any given axial plane equation (5) is

$$\cos \bar{\theta}_j \frac{\partial \psi_{i,j,k}^{g,0}(s,t)}{\partial s} + \tilde{\Sigma}_{tr,m}^g \psi_{i,j,k}^{g,0}(s,t) = \tilde{S}_{i,j,m}^g \quad (6)$$

where, $\bar{\Sigma}_{tr,m}^g$ is the modified transport cross section is defined as,

$$\bar{\Sigma}_{tr,m}^g = \frac{2 \sin \bar{\theta}_j}{\Delta z} + \Sigma_{tr,m}^g$$

and, the total source is defined as

$$\bar{S}_{i,j,m}^{g,0} = \bar{Q}_{ij}^{g,0}(s, t) + \frac{2 \sin \bar{\theta}_j}{\Delta z} \psi_{i,j,k}^{g,-}(s)$$

The analytical solution of Eq. (6) at any time interval,

$$\psi_{out,i,j,k}^{g,0} = \psi_{in,i,j,k}^{g,0} e^{-\bar{\Sigma}_{tr,m}^g t'_{i,j,k}} + \frac{\bar{S}_{i,j,m}^g}{\bar{\Sigma}_{tr,m}^g} \left(1 - e^{-\bar{\Sigma}_{tr,m}^g t'_{i,j,k}} \right) \quad (7)$$

where $\psi_{out,i,j,k}^{g,0}$ is the outgoing angular flux from the ray segment; $\psi_{in,i,j,k}^{g,0}$ is the incoming angular flux to the segment; $t_{i,j,k}$ the length of the segment projected on x-y plane; $t'_{i,j,k}$ is the actual length of segment.

The track average angular flux is defined as,

$$\begin{aligned} \bar{\Psi}_{i,j,k}^{g,0} &= \frac{\int_0^{t'_{i,j,k}} \psi_{i,j,k}^{g,0}(s) ds}{\int_0^{t'_{i,j,k}} ds} \\ &= \frac{\int_0^{t'_{i,j,k}} \left\{ \psi_{i,j,k}^{g,0}(0) e^{-\bar{\Sigma}_{tr,m}^g s} + \frac{\bar{S}_{i,j,m}^g}{\bar{\Sigma}_{tr,m}^g} \left(1 - e^{-\bar{\Sigma}_{tr,m}^g s} \right) \right\} ds}{t'_{i,j,k}} \\ &= \frac{\bar{S}_{i,j,m}^g}{\bar{\Sigma}_{tr,m}^g} + \frac{1}{\bar{\Sigma}_{tr,m}^g t'_{i,j,k}} \left(\psi_{in,i,j,k}^{g,0} - \frac{\bar{S}_{i,j,m}^g}{\bar{\Sigma}_{tr,m}^g} \right) \left(1 - e^{-\bar{\Sigma}_{tr,m}^g t'_{i,j,k}} \right) \quad (8) \end{aligned}$$

The region average angular flux is defined as,

$$\begin{aligned} \bar{\psi}_{i,j,m}^{g,0} &= \frac{\sum_{k \in m} \bar{\Psi}_{i,j,k}^{g,0} t'_{i,j,k} d_i}{\sum_{k \in m} t'_{i,j,k} d_i} \\ &= \sum_{k \in m} \left[\frac{\bar{S}_{i,j,m}^g}{\bar{\Sigma}_{tr,m}^g} + \frac{d_i \cos \theta_j}{\bar{\Sigma}_{tr,m}^g A_m} \left(\frac{\bar{S}_{i,j,m}^g}{\bar{\Sigma}_{tr,m}^g} - \psi_{in,i,j,k}^{g,0} \right) \left(1 - e^{-\bar{\Sigma}_{tr,m}^g t'_{i,j,k}} \right) \right] \quad (9) \end{aligned}$$

where d_i is the ray spacing and A_m is the analytic area of flat source region m.

The flat source region-wise scalar flux is calculated as

$$\phi_m^{g,0} = 4\pi \sum_j \sum_i \bar{\psi}_{i,j,m}^{g,0} \omega_i \omega_j \quad (10)$$

where ω_i and ω_j are the weights for the azimuthal angle and polar angle, respectively.

On the other hand, the delay neutron precursor term can be expressed from equation (3)

$$\frac{dC_k e^{\lambda_k t}}{dt} = e^{\lambda_k t} \beta_k S_F \quad (11)$$

the fission sources at time steps t_n , t_{n-1} and t_{n-2} , we can express the fission source at time t between these time steps using a second order expansion as:

$$\begin{aligned} \beta_k S_F &\approx \beta_k^n S_F^n \frac{\tilde{t}^2 + \tilde{t} \gamma \Delta t_n}{(1+\gamma)(\Delta t_n)^2} + \beta_k^{n-1} S_F^{n-1} \left(1 - \frac{\tilde{t}^2 + (\gamma-1)\Delta t_n \tilde{t}}{\gamma(\Delta t_n)^2} \right) + \beta_k^{n-2} S_F^{n-2} \frac{\tilde{t}^2 - \Delta t_n \tilde{t}}{(1+\gamma)\gamma(\Delta t_n)^2} \quad (12) \\ \tilde{t} &= t - t_{n-1}, \gamma = \frac{\Delta t_{n-1}}{\Delta t_n} \end{aligned}$$

Substituting Eq. (12) to Eq. (11) and integrating from t_{n-1} to t_n yields:

$$\begin{aligned} C_k^n &= \Omega_k^0(\tilde{\lambda}_k^n) C_k^{n-1} + \frac{1}{\lambda_k^n} \left(\beta_k^n S_F^n \Omega_k^n(\tilde{\lambda}_k^n) + \beta_k^{n-1} S_F^{n-1} \Omega_k^{n-1}(\tilde{\lambda}_k^n) + \beta_k^{n-2} S_F^{n-2} \Omega_k^{n-2}(\tilde{\lambda}_k^n) \right) \quad (13) \end{aligned}$$

where,

$$\tilde{\lambda}_k^n = \lambda_k^n \Delta t_n, E(x) = e^{-x},$$

$$k_0(x) = 1 - e^{-x}, \gamma = \frac{\Delta t_{n-1}}{\Delta t_n}$$

$$k_1(x) = 1 - \frac{k_0(x)}{x}, k_2(x) = 1 - \frac{2k_1(x)}{x}$$

$$\Omega_k^0(\tilde{\lambda}_k^n) = E(\tilde{\lambda}_k^n)$$

$$\Omega_k^n(\tilde{\lambda}_k^n) = \frac{k_2(\tilde{\lambda}_k^n) + \gamma k_1(\tilde{\lambda}_k^n)}{(1+\gamma)}$$

$$\Omega_k^{n-1}(\tilde{\lambda}_k^n) = k_0(\tilde{\lambda}_k^n) - \frac{k_2(\tilde{\lambda}_k^n) + (\gamma-1)k_1(\tilde{\lambda}_k^n)}{\gamma}$$

$$\Omega_k^{n-2}(\tilde{\lambda}_k^n) = \frac{k_2(\tilde{\lambda}_k^n) - k_1(\tilde{\lambda}_k^n)}{(1+\gamma)\gamma}$$

The delay neutron source term can be expressed by

$$\begin{aligned} S_d^{m,n} &= \sum_{k=1}^K \lambda_k C_k^{m,n-1} e^{-\lambda_k \Delta t_n} + \\ \sum_{l=n-2}^n \sum_{k=1}^K \beta_k^m \Omega_k^{m,l} S_F^{m,l} &= \tilde{S}_d^{m,n-1} + \omega^{m,n} S_F \quad (14) \end{aligned}$$

where, $\omega^n = \sum_{k=1}^K \beta_k \Omega_k^n(\tilde{\lambda}_k^n)$

$$\begin{aligned} \tilde{S}_d^{n-1} &= \sum_{k=1}^K \lambda_k \Omega_k^0(\tilde{\lambda}_k^n) C_k^{n-1} + S_F^{n-1} \sum_{k=1}^K \beta_k^{n-1} \Omega_k^{n-1}(\tilde{\lambda}_k^n) \\ &\quad + S_F^{n-2} \sum_{k=1}^K \beta_k^{n-2} \Omega_k^{n-2}(\tilde{\lambda}_k^n) \end{aligned}$$

In CMFD, time-dependent continuous diffusion and corresponding precursor equation are used in the coarse mesh. In every course mesh homogenized condensed parameters are calculated from the MOC cell.

For a given time step size Δt_n at time step n, equation (1) can be discretized using the theta method as:

$$\begin{aligned} \frac{1}{\theta \Delta t_n} (\psi_{i,j,k}^{g,0,n} - \psi_{i,j,k}^{g,0,n-1}) &= \theta R_g^{m,n} + (1 - \theta) R_g^{m,n-1} \quad (15) \end{aligned}$$

where, $R_g^{m,n}$ is the right side of equation (1) and θ represent the numerical solution scheme. STREAM use $\theta = 0.5$ which imply the Crank-Nicholsen scheme.

2. Numerical Results

2.1 TWIGL 2G problem

TWIGL [3,4] benchmark is a simple quarter-symmetric reactor core with three homogeneous regions as shown in Fig. 1. The initial state, regions 1, 2 and 3 of the reactor use material composition 1, 2 and 3 respectively [material composition is given ref. 4]. The core region 1 material composition is perturbed as describe in Table 1 and Region 3 is in the core center and peripheries. The radial core size is 80 cm. The reactor South and West side used reflective boundary condition alternatively North and East side used zero incoming current boundary condition. Two neutron energy groups and single precursor group are used in this problem. TWIGL problem was run using fixed time steps (5 ms and 10 ms) and compared the obtained by the DeCARD code [4]. Which used theta method with the addition of adaptive time stepping. STREAM used a ray spacing of 0.02 cm, 96 azimuthal with 6 polar angles.

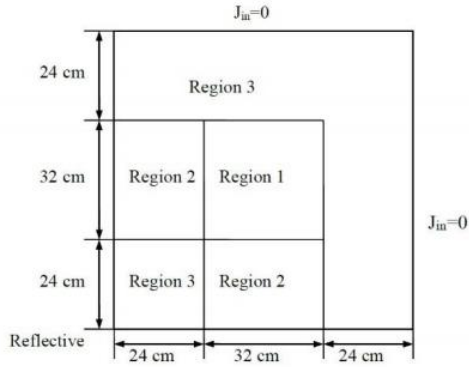


Fig. 1. Geometry for the TWIGL 2G benchmark problem

Table 2 shows the steady state k-effective of STREAM with different code. Time step size 10 ms was used to simulate 0.5 s and total 30 minute required by using single thread (core) (1.1 hr. for 5 ms time step). Fig. 2 shows the total core power history throughout the transient. A comparison of several power; including peak and asymptotic is shown in Table 3. The total core power increases up to about 2.2 times at 0.2 second according to the decrease in the capture cross section in region 1. After then, the increase of capture cross section again the core power start decreasing and fall to about 0.65 times at 0.4 second. Finally, the capture cross section return to its initial state at 0.4 s and the transient core power recovers its initial power.

Table 1: Transient perturbations for the TWIGL problem

Initial		Final		Perturb.
Time (s)	material	Time (s)	material	
0.0	1	0.2	4	Linear change
0.2		0.200001	5	Step change
0.200001		0.4	6	Linear change
0.4		0.400001	1	Step change

Table 2: Steady State (Initial) k-effective for TWIGL

Code	k-effective
DeCARD	0.91605
STREAM	0.91597

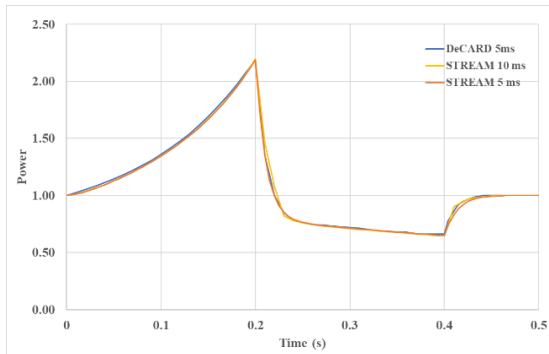


Fig. 2: Power history of TWIGL 2G problem

Table 3: Region wise pin power comparisons for TWIGL

Time (s)	Region	STREAM	DeCART	Error*
0.0	1	1.5701	1.5699	0.01%
	2	1.9938	1.9935	0.02%
	3	0.4504	0.4506	-0.04%
0.1	1	1.5937	1.5937	0.00%
	2	1.9819	1.9815	0.02%
	3	0.4489	0.4491	-0.04%
0.2	1	1.6183	1.6183	0.00%
	2	1.9693	1.9690	0.02%
	3	0.4474	0.4475	-0.02%
0.3	1	1.5364	1.5363	0.00%
	2	2.0113	2.0109	0.02%
	3	0.4525	0.4526	-0.03%
0.4	1	1.5257	1.5255	0.01%
	2	2.0168	2.0165	0.01%
	3	0.4531	0.4533	-0.04%
0.5	1	1.5699	1.5699	0.00%
	2	1.9938	1.9935	0.02%
	3	0.4504	0.4506	-0.03%

* error = 100 - 100*sol.(DeCART)/sol.(STREAM)

Table 4: Power comparisons for TWIGL

	$\Delta t=10$ ms	$\Delta t=5$ ms	Ref.
Peak Power	2.195	2.189	2.183
Asymptotic Power	1.002	1.002	1.002

2.2 C5G7 problem

C5G7 benchmark [5,6] is a miniature light water reactor (LWR) with sixteen fuel assemblies (minicore): eight uranium oxide (UO₂) assemblies and eight mixed oxide (MOX) assemblies, surrounded by a water reflector. Both UO₂ and MOX assemblies follow the 17×17 configuration, consisting of 264 fuel pins, 24 guide tubes for control rods and one instrument tube for a fission chamber in the center grid-cell. All pin cells have a pin radius of 0.54 cm with a pitch of 1.26 cm. The MOX assemblies have three enrichments of 4.3%, 7.0%, and 8.7%. The benchmark provided the transport corrected few-group cross sections and scattering matrices in seven-group structure for UO₂, MOX (three enrichments), the guide tubes and fission chamber, and the moderator. All cross sections were provided for all the pin cells in a simplified 2-region geometry, where “Outer cell” represents the moderator outside and “Inner cell” refers to the mixture of all medium surrounded by “Outer cell”. The 3-D geometry as shown in Fig. 3 is adopted with minor modifications, primarily on the axial core configuration. The height of the fuel assembly is increased to 128.52 cm with additional 21.42 cm-thick upper and lower axial reflector. Vacuum boundary condition has been applied to the axial boundary of the core so that control rods can only be inserted from the top.

In STREAM, the mesh for each pin cell consists of 3 radial rings for the inner zone, 3 radial rings for the

outer zone and one azimuthal mesh for each half-face (1/8 of the square cell). The mesh for each pin-cell-equivalent sub-region of the reflector is a 5x5 grid. In total, the 2-D mesh contains 91,613 elements and the 3-D configuration, the 2-D mesh was extruded using 24 axial planes. MOC ray was performed using 0.05 cm spacing with 6 polar angles and 48 azimuthal angles. The eigenvalue results from STREAM is shown in Table 5 with the reference result from Ref..

Table 5: Eigenvalue for the C5G7-TD 3-D benchmarks.

Code	3-D Eigenvalue
MPACT	1.16351
PROTEUS-MOC	1.16469
STREAM	1.16543

The 3-D problems contain two distinct problems: Control rod insertion/withdrawal and another one the moderator density variation. Each of them contains sub-problems. In exercise 5 (TD5), A linear decrease in water density, varying by location, followed by returning to original density.

Instead of the insertion and withdrawal of the control rods, exercise TD5 is based on the density variation of the moderators. All control rods in this exercise are located in the fully un-rodded configuration. There are 4 sub-problems differentiated by the magnitude of density change in moderator in different fuel assemblies taken from reference [7]. The change of transient power level changes with time for TD5 exercise is shown in Fig. 4. 25 ms time step is used for this calculation. Twenty number of threads (cores) is used to simulate the problem and the run time summary is listed in Table 6.

Table 6: Run time summary for TD5 (10 s transient)

TD5-1	TD5-2	TD5-3	TD5-4
29.32h	33.04h	29.03h	32.54h

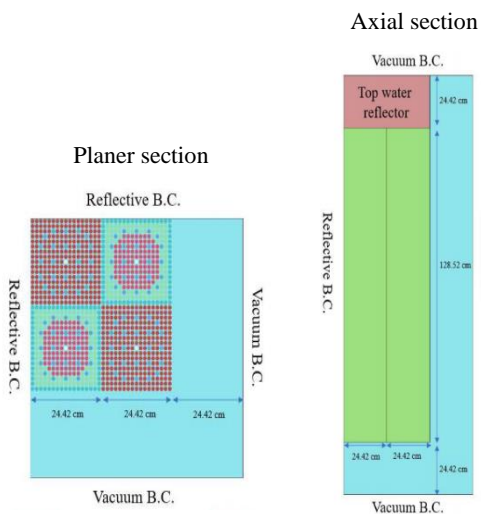


Fig. 3: Modified 3-D configuration for the benchmark

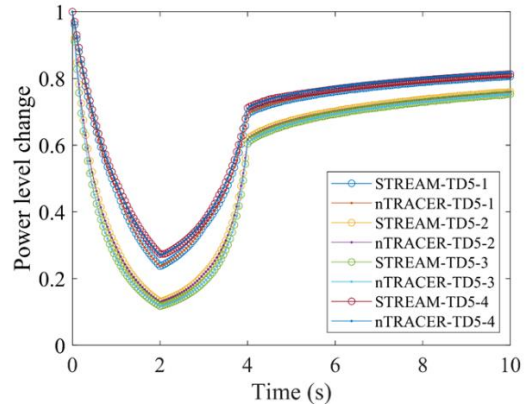


Fig. 4: TD5 core fission rate

3. Conclusions

The simulation of transient benchmark with two problems was performed with STREAM to continue the verification and validation of the transient capability. A density change of the moderator is used in 3-D problem whereas perturbed the absorption cross section of the material in 2-D problem. Agreement with STREAM shows good results in comparison with other code. However more benchmark simulation required to improve the accuracy of the code. Finally, it provides a valuable contribution to the verification of the transient methods used in STREAM.

4. Acknowledgement

This work was supported by the National Research Foundation of Korea (NRF) grant funded by the Korea government (MSIT). (No. NRF2019M2D2A1A03058371).

REFERENCES

- [1] Sooyoung Choi, Deokjung Lee, "Three-dimensional method of characteristics/diamond-difference transport analysis method in STREAM for whole-core neutron transport calculation", Computer Physics Communications, 28 April 2020, 107332.
- [2] Sooyoung Choi, Changho Lee, Deokjung Lee, "Resonance Treatment using Pin-Based Pointwise Energy Slowing-Down Method," J. Comput. Phys., 330: 134-155. (2017)
- [3] "The numerical nuclear reactor for high fidelity integrated simulation of neutronics, thermal-Hydraulic and Thermo-Mechanical Phenomena, Final Report." International Nuclear Energy Research Initiative, Project Number 2002-010-K (2005).
- [4] Transient Capability of the DeCART Code, Korea Atomic Energy Research Institute, KAERI/TR-2930/2005.
- [5] M. A. Smith, E. Lewis and B.-C. Na, "Benchmark on Deterministic Transport Calculations Without Spatial Homogenization (MOX Fuel Assembly 3-D Extension Case)," Organization for Economic CoOperation and Development/Nuclear Energy Agency Report NEA, 2005.
- [6] Victor F. Boyarinov and Peter A. Fomichenko, "Deterministic Time-Dependent Neutron Transport Benchmark without Spatial Homogenization (C5G7-TD)" Volume I: Kinetics Phase, Organization for Economic CoOperation and Development/Nuclear Energy Agency Report NEA, 2018.